EPJ Web of Conferences **3**, 03029 (2010)
DOI:10.1051/epjconf/20100303029

nd Scattering Observables Predicted by the Quark-Model Baryon-Baryon Interaction

Y. Fujiwara[1,a] and K. Fukukawa[1]

Department of physics, Kyoto University, Kyoto 606-8502, Japan

Abstract. We solve the *nd* scattering in the Faddeev formalism, employing the *NN* sector of the quark-model baryon-baryon interaction fss2. The energy-dependence of the *NN* interaction, inherent to the (3*q*)-(3*q*) resonating-group formulation, is eliminated by the standard off-shell transformation utilizing the $1/\sqrt{N}$ factor, where *N* is the normalization kernel for the (3*q*)-(3*q*) system. This procedure yields an extra nonlocality, whose effect is very important to reproduce all the scattering observables below $E_n \leq 65$ MeV. The different off-shell properties from the standard meson-exchange potentials, related to the non-locality of the quark-model baryon-baryon interaction, yields appreciable effects to the differential cross sections and polarization observables of the *nd* elastic scattering, which are usually attributed to the specific properties of three-body forces.

1 Introduction

The QCD-inspired spin-flavor SU_6 quark model (QM) for the baryon-baryon interaction, developed by the Kyoto-Niigata group, has achieved accurate description of available nucleon-nucleon (*NN*) and hyperon-nucleon experimental data [1]. These QM baryon-baryon interactions are characterized by the nonlocality and the energy dependence inherent to the framework of the resonating-group method (RGM) for two three-quark systems. In the strangeness sector, the Pauli forbidden state sometimes exists as the result of the exact antisymmetrization of six quarks. The short-range repulsion of the baryon-baryon interaction is mainly described by the quark-exchange kernel, which gives quite different off-shell properties from the standard meson-exchange potentials. The energy dependence of the interaction is eliminated [2] by the standard off-shell transformation, utilizing the $1/\sqrt{N}$ factor for the interaction Hamiltonian and the renormalized relative wave function between two clusters. This procedure yields an extra nonlocality, whose effect was examined in detail for the three-nucleon bound state and for the hypertriton [3]. The advantage of the larger triton binding energy by the QM *NN* interaction; namely, the deficiency of 350 keV, predicted by the model fss2, is still much smaller than the standard values 0.5 MeV - 1 MeV, given by the modern meson-exchange *NN* potentials. It is therefore interesting to examine the QM predictions to the three-nucleon scattering observables, especially in this renormalized framework without the explicit energy dependence of the RGM kernel.

In this contribution, we apply our QM *NN* interaction fss2 to the neutron-deuteron (*nd*) scattering in the Faddeev formalism for composite systems [4]. The Alt-Glassberger-Sandhas (AGS) equations are solved in the momentum representation, using the off-shell RGM *T*-matrix obtained from the energy-independent renormalized RGM kernel [2]. The Gaussian nonlocal potentials constructed from the fss2 is essentially used in the isospin basis. The singularity of the *NN T*-matrix from the deuteron pole is handled in the Noyes-Kowalski method. Another notorious moving singularity of the free three-body Green function is treated by the the standard spline interpolation technique developed by the Böchum group [5]. We use the channel-spin formalism which is convenient to discuss the *nd* scattering. The *NN* interaction up to $I_{\max} = 4$ is included in the present calculations up to about $E_n = 65$ MeV.

In order to confirm the importance of the present off-shell transformation, we have also calculated the differential cross sections and various types of analyzing powers, the polarization transfer, and spin correlation parameters, using a simple prescription of assuming a constant energy of two-nucleon subsystem; namely, the deuteron energy, $\varepsilon = -\varepsilon_d = -2.223$ MeV. In this prescription, we come across some disagreements with experimental data. Only when the off-shell transformation is properly taken into account, we can achieve an overall agreement with experiment. We therefore show in this paper only the results obtained with the renormalized RGM kernel of the QM BB interaction.

2 *NN* phase shifts predicted by fss2

We show in Fig. 1 the *NN* phase shifts predicted by the model fss12. More detailed information on the QM BB interaction is obtained from the QMPACK homepage [6].

The energy-independent renormalized RGM kernel $V^{\rm RGM}$ for a two-cluster system reads [2]

[a] e-mail: yfujiwar@scphys.Kyoto-u.ac.jp

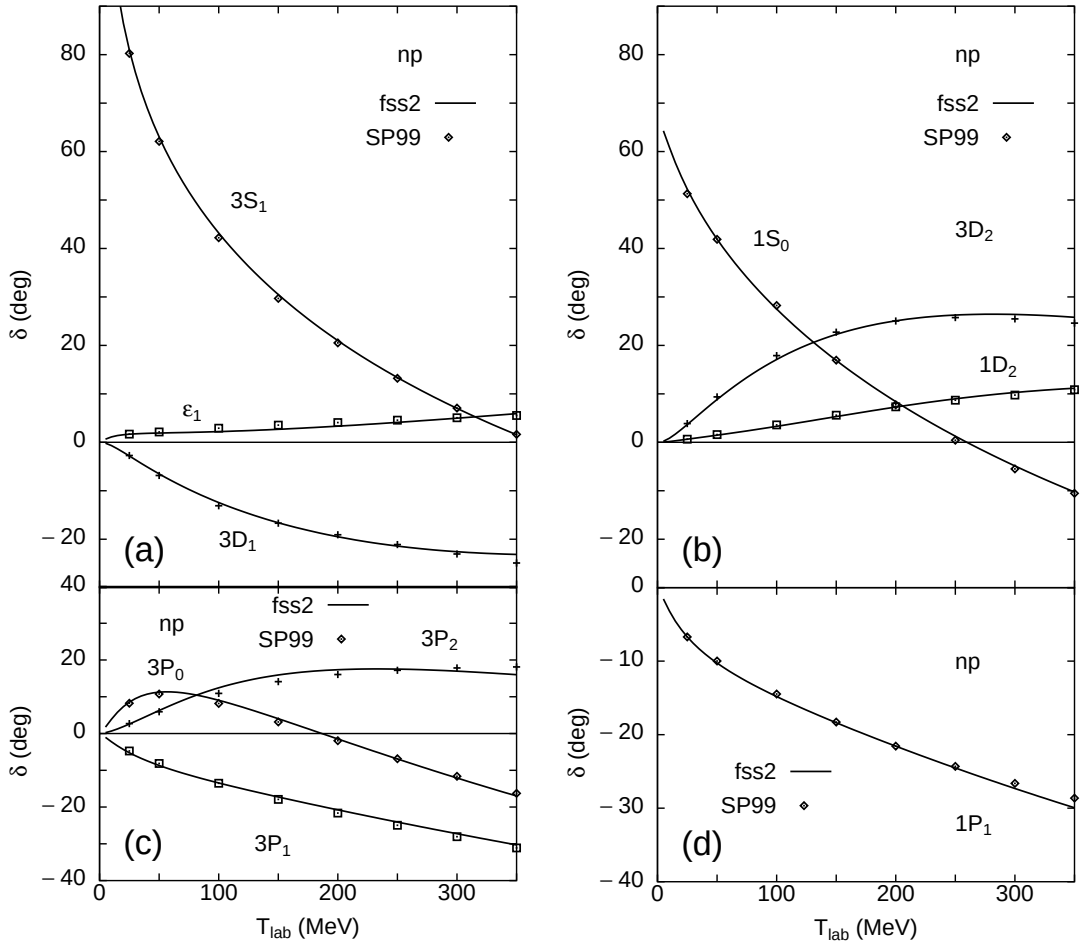

Fig. 1. Calculated *np* phase shifts by fss2 in the isospin basis, compared with the phase-shift analysis SP99 by Arndt *et al.* [7]

$$V^{\rm RGM} = V_{\rm D} + G + W \,, \tag{1}$$

where $V_{\rm D}$ is the direct potential, and G is the sum of the exchange kinetic-energy and interaction kernels. The nonlocal kernel W appears through the elimination of the energy-dependence, and is given by

$$W = \Lambda \frac{1}{\sqrt{1-K}} h \frac{1}{\sqrt{1-K}} \Lambda - h \,. \tag{2}$$

Here K is the exchange normalization kernel, h denotes $h_0 + V_{\rm D} + G$ with h_0 being the kinetic energy for the two-cluster relative motion, and $\Lambda = 1 - |u\rangle\langle u|$ is a two-cluster Pauli projection operator, where $|u\rangle$ is a Pauli-forbidden state satisfying $K|u\rangle = |u\rangle$. In the NN sector, there appears no Pauli forbidden state at the quark level, so that we can simply set $\Lambda = 1$ in the following formulations. An advantage of using the $V^{\rm RGM}$ is that the two-cluster RGM equation takes the form of the usual Schrödinger equation in the Pauli-allowed model space, and the relative wave function is properly normalized. This Schrödinger-type equation for the relative wave function gives the same asymptotic behavior as the original RGM equation, thus preserving the phase shifts and physical observables for the two-cluster system. The difference between the previous energy-dependent RGM kernel, $V^{\rm RGM}(\varepsilon) = V_{\rm D} + G + \varepsilon K$ [4], and $V^{\rm RGM}$ in Eq. (1) is essentially a replacement of $\Lambda(\varepsilon K)\Lambda$ with W. Here ε is the two-cluster relative energy measured from its threshold. The value is however not defined in the three-cluster system, in particular, for the scattering systems. In the following, we will consistently use the energy-independent renormalized RGM kernel $V^{\rm RGM}$ in Eq. (1), both for the bound-state solution and the scattering problems.

3 Three-nucleon bound state

The three-cluster equation for the $3N$ bound state reads

$$\left[E - H_0 - V_\alpha^{\rm RGM} - V_\beta^{\rm RGM} - V_\gamma^{\rm RGM} \right] \Psi = 0 \,, \tag{3}$$

where α, β, and γ denote three independent pairs of two-cluster subsystems, H_0 is the free three-body kinetic-energy operator, and $V_\alpha^{\rm RGM}$ stands for the RGM kernel in Eq. (1) for the α-pair, *etc.*

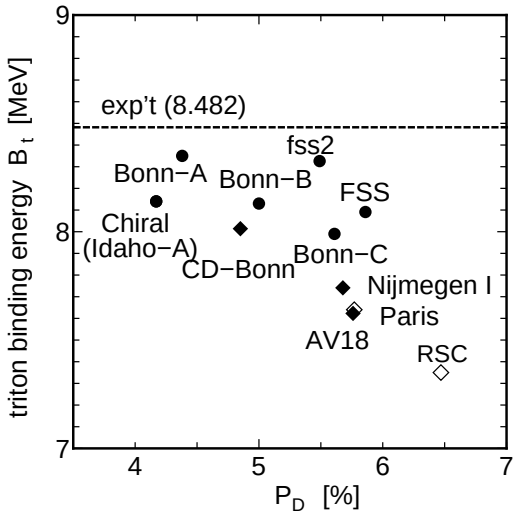

Fig. 2. Calculated ^{3}H binding energies B_t as a function of the deuteron D-state probability P_D. Calculations are made in the isospin basis, using the np interaction, for fss2, FSS, Bonn-A, B, C and Chiral (denoted by black circles). The group, including CD-Bonn, Nijmegen I and AV18 (denoted by black diamonds), takes into account the effect of charge-dependence of the interaction. In the Paris and RSC results (denoted by the open diamonds), the $^1S_0$ interaction is determined from the pp scattering data. Those energies denoted by black circles go down by about 190 keV when the charge dependence of the NN force is taken into account. The experimental value, B_t = 8.482 MeV, is shown by the dashed line.

The correlation between the triton binding energy, $B_t = -E(^3\mathrm{H})$, and the D-state probability of the deuteron is plotted in Fig. 2 for fss2 and FSS, as well as many other Faddeev calculations using modern realistic meson-exchange potentials. In the traditional meson-exchange potentials, the calculated points are located on a straight line, which is similar to the Coester line for the saturation point of symmetric nuclear matter. We find that fss2 gives a larger binding energy than the modern realistic meson-exchange potentials like Bonn-C and AV18, while the result of FSS is not very far from that of Bonn-C. It is interesting to note that our QM points are apparently off the line on which the data points of the modern meson-exchange potentials fall. By taking into account the charge-dependence correction of 190 keV, we conclude that the quark-model potential underbinds the triton by approximately 350 keV [3]. Thus the energy to be accounted for by three-nucleon forces may not be as large as 0.5 - 1 MeV, which most of standard meson-exchange potentials [8] predict. The different predictions for the contributions of the three-body force prompt us to examine what results the present quark-model NN interaction produces in other three-nucleon observables, especially in the nd and pd scatterings.

4 Effective range parameters

The accurate calculation of the effective range parameters of the nd scattering is very difficult especially for the spin-doublet ($S_c = 1/2$) channel, because of the pole structure of $k\cot\delta$ near the zero-energy threshold. We apply an extended effective range expansion

$$k\cot\delta = \frac{-\frac{1}{a} + \frac{1}{2}rk^2}{1 + \frac{k^2}{{k_0}^2}}\ , \tag{4}$$

in this particular case. We have obtained $^2a = 0.60$ fm for $I_{\max} = 4$ with a pole located at $E = -(\hbar^2/2\mu){k_0}^2 = -130$ keV. Here, $I_{\max}$ is the maximum value of the NN total angular momentum included in the calculation. This value of the doublet scattering length is comparable with the experimental value $^2a^{\mathrm{exp}} = 0.65 \pm 0.04$ fm. On the other hand, the quartet scattering length is almost independent of the model space truncation, and is well reproduced as $^4a = 6.27$ fm vs. $^4a^{\mathrm{exp}} = 6.35 \pm 0.02$ fm. We compare our results with some predictions by meson exchange potentials in Table 1. Note that the charge dependence of the NN interaction is neglected in our calculation, but the effect is rather small. We find that the fss2 results almost reproduce the experimental values of $E_B(^3\mathrm{H})$, ^2a, and ^4a, without reinforcing the two-body NN force with the three-body forces.

5 Total cross sections

The elastic and breakup total cross sections up to 40 MeV, predicted by fss2, are plotted in Fig. 3, together with the experimental data. Although the experimental values of total breakup cross sections have large error bars especially at the low-energy region, the elastic and total cross sections are nicely reproduced based on the constraint of the optical theorem.

6 Differential cross sections and polarizations

We have examined the elastic differential cross sections ($d\sigma/d\Omega$), the neutron analyzing power $A_y(\theta)$, and deuteron vector ($iT_{11}(\theta)$) and tensor ($T_{2m}(\theta)$) analyzing powers up to about $E_n = 65$ MeV at the moment. We show some typical results in Figs. 4 - 9. More complex polarization observables including the nucleon polarization transfer $K_\alpha{}^{\beta'}(\theta)$, the nucleon to deuteron polarization transfer $K_\alpha{}^{\beta'}(\theta)$ and $K_\alpha{}^{\beta'\gamma'}(\theta)$, and the spin correlation coefficients $C_{\alpha\beta}(\theta)$ and $S(\theta) = (-1/2)C_y{}^{yy}(\theta)$, are found in the QMPACK homepage [6].

The salient features of the obtained results are as follows:

1. The minimum values of the differential cross sections have an opposite energy dependence to the one given by the standard meson-exchange potentials. For the QM

Table 1. The *nd* scattering length predicted by fss2 (I_{max} = 4 with n=8-8-8). For fss2 results, the charge dependence of the *NN* force is neglected. The heading *NN* implies the calculation only by the two-nucleon force, and *NN*+TM including the three-nucleon force. The results by CD-Bonn 2000, AV18, and Nijm I, are taken from [9].

model	$E_B(^3\mathrm{H})$ (MeV)		$^2a_{nd}$ (fm)		$^4a_{nd}$ (fm)
	NN	*NN*+TM	*NN*	*NN*+TM	*NN*(+TM)
fss2	−8.307	—	0.60	—	6.27
CD-Bonn 2000	−7.946	−8.419	0.976	0.622	6.347
AV18	−7.569	−8.478	1.304	0.614	6.346
Nijm I	−7.742	−8.493	1.158	0.601	6.342
exp	−8.482		0.65 ± 0.04		6.35 ± 0.02

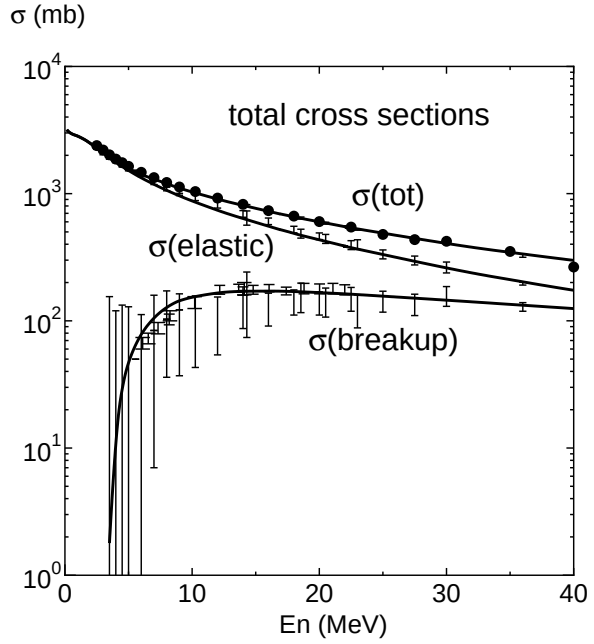

Fig. 3. The fss2 predictions to the *nd* total cross sections up to E_n = 40 MeV, compared with the experiment.

NN interaction, the cross section minima are higher for higher energies. This behavior of the differential cross sections is consistent with the bound-state calculation of ^{3}H, in which fss2 predicts a large binding energy close to the experiment without introducing any three-body forces.

2. A slight overestimation of the differential cross sections is developing at forward angles when the energy becomes higher than $E_n \sim 35$ MeV. (See Fig. 5.) This overestimation is not improved by the renormalized RGM prescription of the QM interaction. Although the correct treatment of the W term in Eq. (1) is important, the effect of an extra nonlocality from this prescription may not be so large.
3. The maximum height of the neutron analyzing power $A_y(\theta)$ in $E_n \leq 20$ MeV (the so-called A_y puzzle) is improved and is almost similar to the old results by the separable approximation of the realistic *NN* potentials. However, there still remains the deficiency of the order of 10%. (See Fig. 6.) On the other hand, the vector-type deuteron analyzing power $iT_{11}(\theta)$ is generally well reproduced. (See Fig. 7.) The tensor-type deuteron analyzing power $T_{2m}(\theta)$ in Fig. 8 seems to imply the importance of the Coulomb effect even at the energy $E_n \sim 9$ MeV [10, 11].

7 Summary

We have applied our quark-model *NN* interaction fss2 to the neutron-deuteron (*nd*) scattering in the Faddeev formalism for composite systems. The energy-dependence of the (3q)-(3q) RGM kernel is eliminated by the standard off-shell transformation utilizing the $1/\sqrt{N}$ factor, where N is the normalization kernel for the (3q)-(3q) system. This procedure yields an extra nonlocality, whose effect is very important to reproduce all the scattering observables below $E_n \leq 65$ MeV. We have found many new features which seem to be related to the different off-shell properties possessed by the quark-model baryon-baryon interaction. These include: 1) a large triton binding energy, 2) reproduction of the doublet scattering length ^2a, 3) the energy dependence of the differential cross sections at the minimum points, 4) the maximum hight of the nucleon analyzing power $A_y(\theta)$ in the low-energy region $E_n \leq 20$ MeV. We are now investigating the observables related to the deuteron breakup processes.

Acknowledgments

This work was supported by the Grant-in-Aids for Scientific Research on Priority Areas (Grant No. 20028003), and by the Grant-in-Aid for the Global COE Program "The Next Generation of Physics, Spun from Universality and Emergence" from the Ministry of Education, Culture, Sports, Science and Technology (MEXT) of Japan. The numerical calculations were carried out on Altix3700 BX2 at YITP in Kyoto University.

References

1. Y. Fujiwara, Y. Suzuki, and C. Nakamoto, Prog. Part. Nucl. Phys. **58**, (2007) 439.

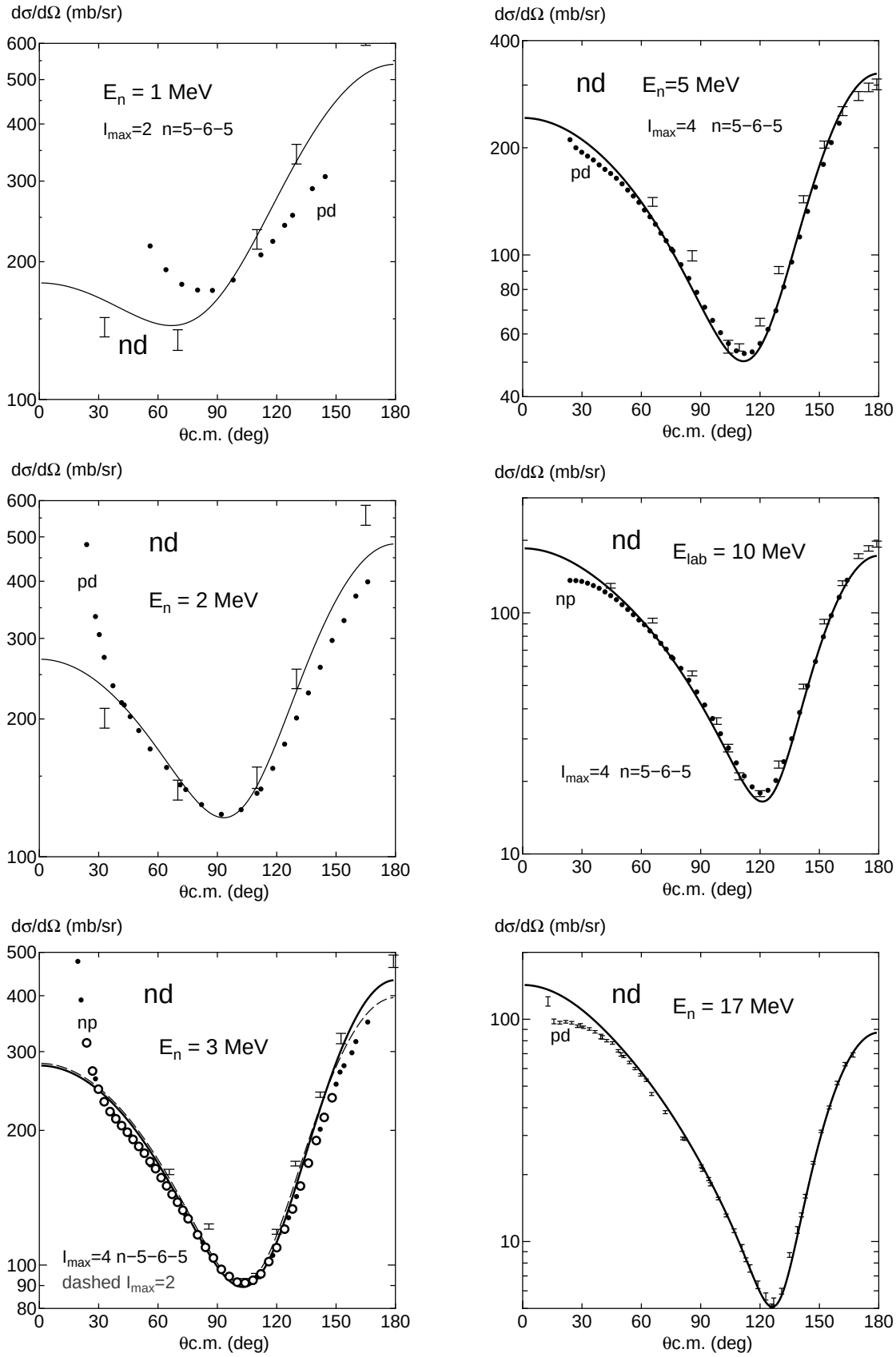

Fig. 4. The *nd* differential cross sections from E_n = 1 MeV to E_n = 17 MeV, compared with the experiment.

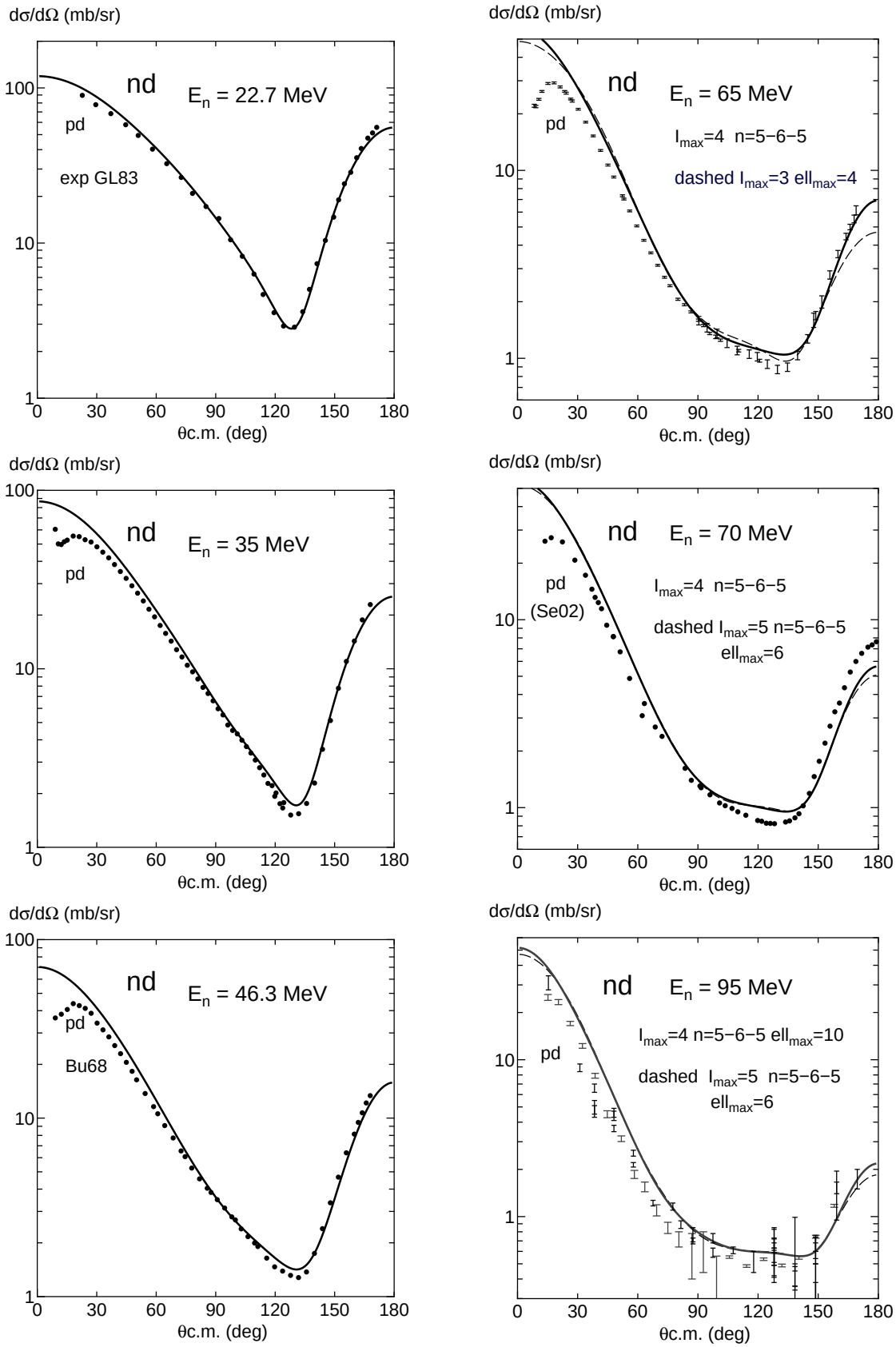

Fig. 5. The *nd* differential cross sections from E_n = 22.7 MeV to E_n = 95 MeV, compared with the experiment.

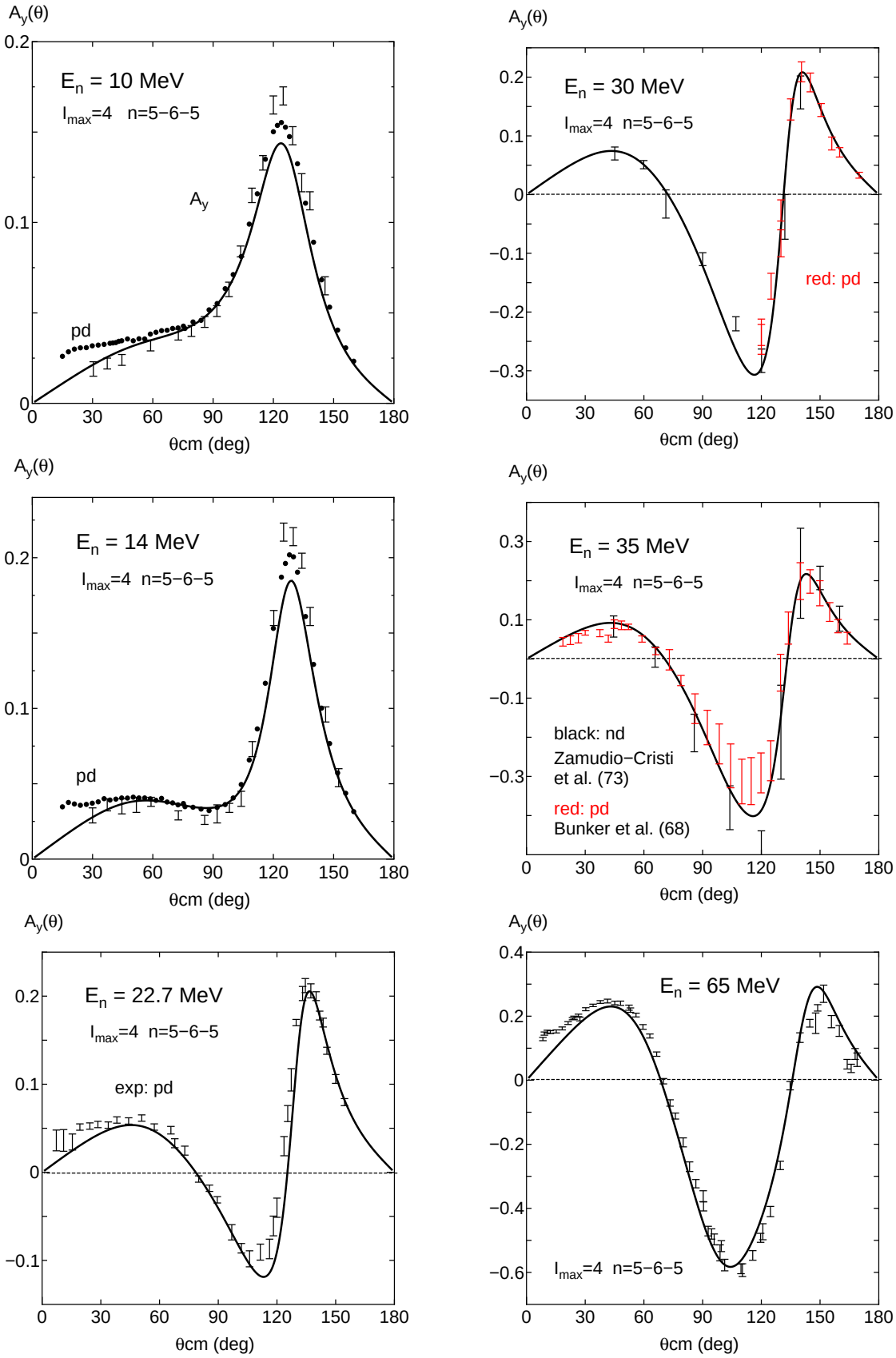

Fig. 6. The nucleon analyzing power $A_y(\theta)$ from E_n = 10 MeV to E_n = 65 MeV, compared with the experiment.

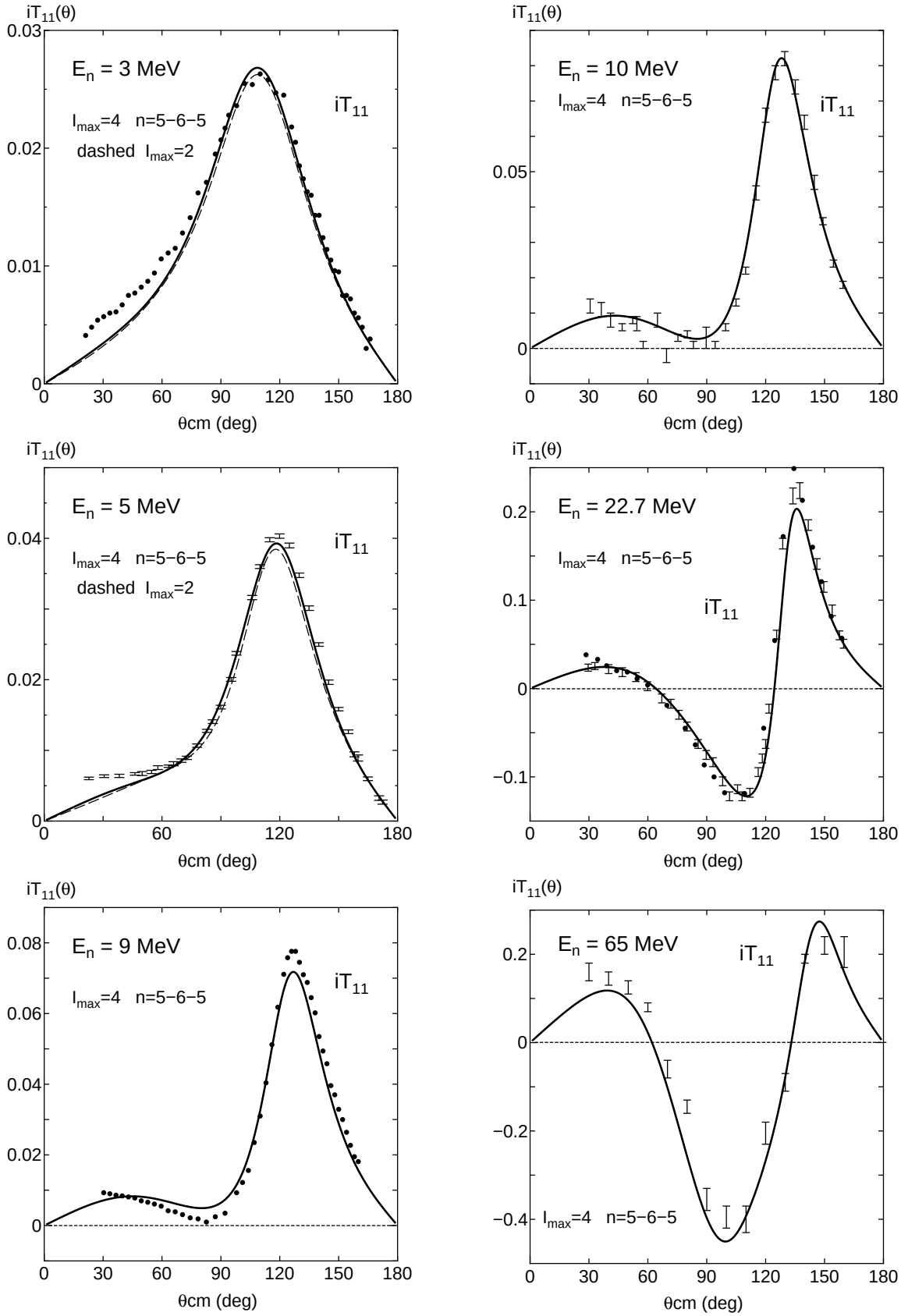

Fig. 7. The vector-type deuteron analyzing power $iT_{11}(\theta)$ from $E_n = 3$ MeV to $E_n = 65$ MeV, compared with the experiment.

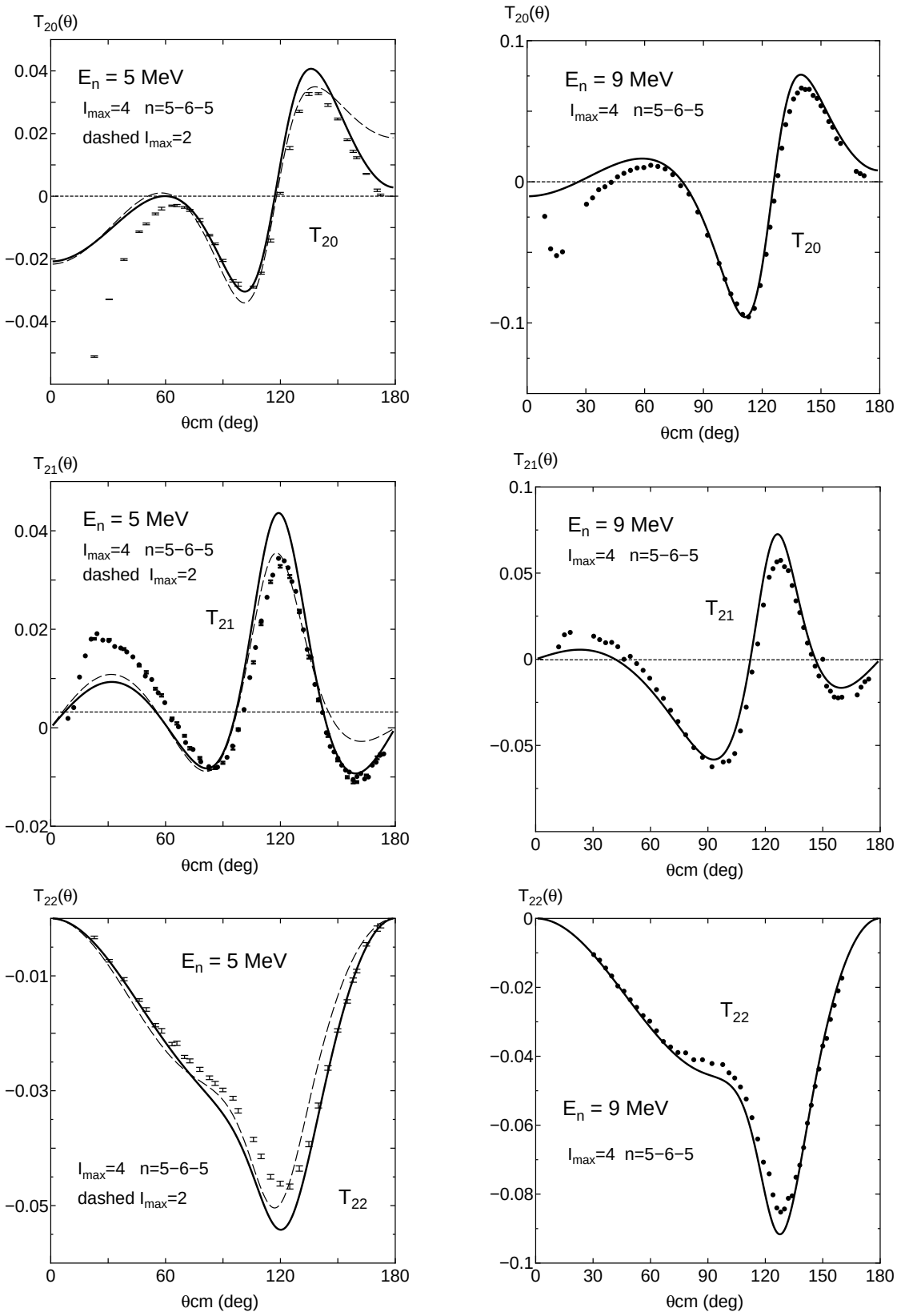

Fig. 8. The tensor-type deuteron analyzing power $T_{2m}(\theta)$ at $E_n = 5$ MeV (left panels) and at $E_n = 9$ MeV (right panels), compared with the experiment.

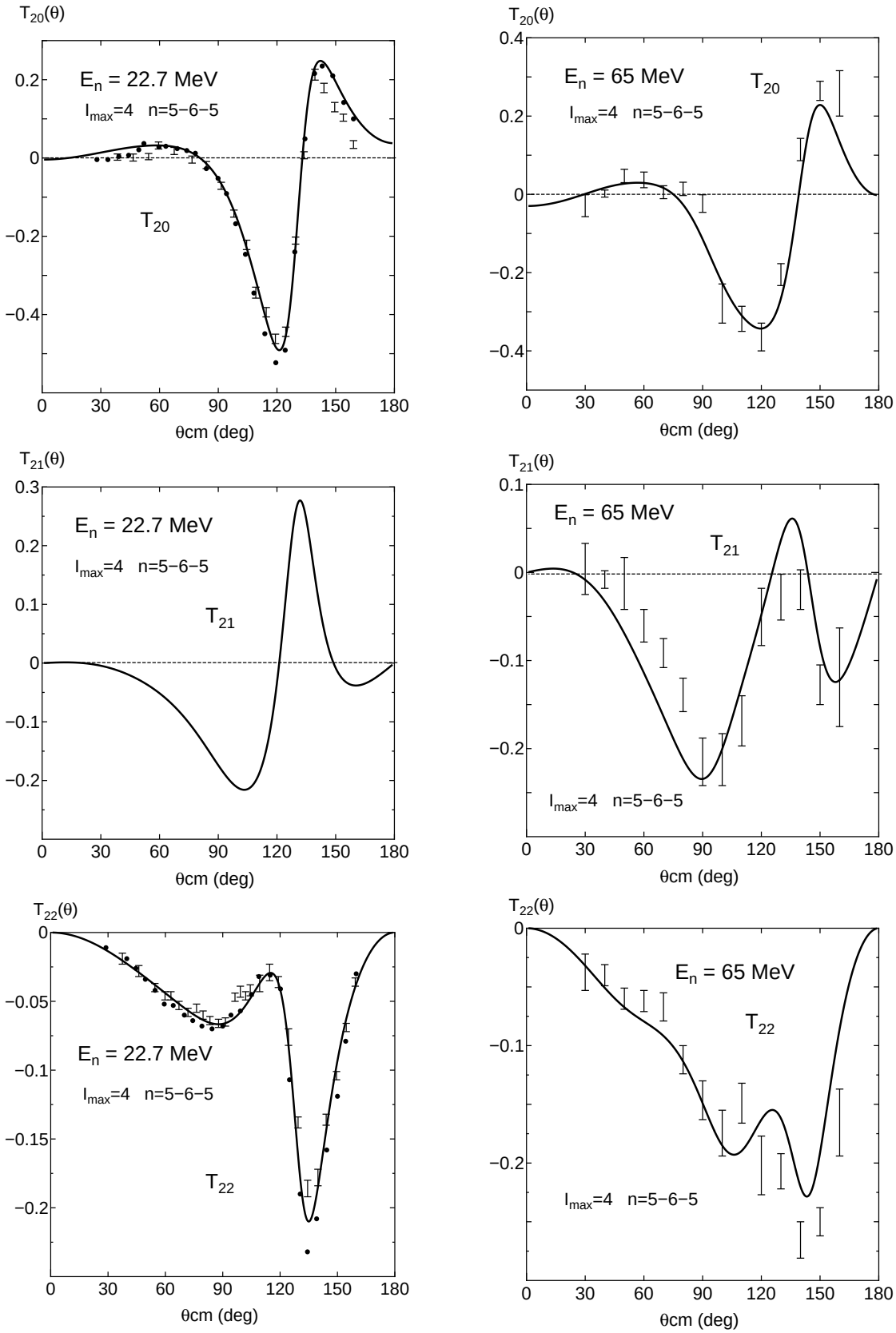

Fig. 9. The tensor-type deuteron analyzing power $T_{2m}(\theta)$ at E_n = 22.7 MeV (left panels) and at E_n = 65 MeV (right panels), compared with the experiment.

2. Y. Suzuki, H. Matsumura, M. Orabi, Y. Fujiwara, P. Descouvemont, M. Theeten and D. Baye, Phys. Lett. **B659** (2008) 160.
3. Y. Fujiwara, Y. Suzuki, M. Kohno, and K. Miyagawa, Phys. Rev. C **66**, 021001 (R)(2002); *ibid.* **70**, 024001 (2004); **77**, 027001 (2008).
4. Y. Fujiwara *et al.*, Prog. Theor. Phys. **107**, 745 (2002); *ibid.* **107**, 993 (2002).
5. H. Witala, Th. Cornelius, and W. Glöckle, Few-Body Systems **3** (1988) 123.
6. http://qmpack.homelinux.com/~qmpack/index.php
7. Scattering Analysis Interactive Dial-up (SAID), Virginia Polytechnic Institute, Blacksburg, Virginia, R. A. Arndt: Private Communication.
8. A. Nogga and H. Kamada and W. Glöckle, Phys. Rev. Lett. **85**, 944 (2000).
9. H. Witala *et al.*, Phys. Rev. C **68**, 034002 (2003).
10. A. Deltuva, A. C. Fonseca, and P. U. Sauer, Phys. Rev. C **71**, 054005 (2005).
11. S. Ishikawa, Private Communication.